



Engineered *Bdellovibrio bacteriovorus* enhances antibiotic penetration and biofilm eradication

Ying Tang^a, Yang Chen^a, Yong-Dan Qi^b, Hui-Yi Yan^a, Wen-An Peng^a, Yu-Qiang Wang^a, Qian-Xiao Huang^b, Xin-Hua Liu^b, Jing-Jie Ye^b, Yun Yu^b, Xian-Zheng Zhang^{b,*}, Cui Huang^{a,*}

^a State Key Laboratory of Oral & Maxillofacial Reconstruction and Regeneration, Key Laboratory of Oral Biomedicine Ministry of Education, Hubei Key Laboratory of Stomatology, School & Hospital of Stomatology, Wuhan University, Wuhan 430079, PR China

^b Key Laboratory of Biomedical Polymers of Ministry of Education & Department of Chemistry, Wuhan University, Wuhan 430072, PR China

ARTICLE INFO

Keywords:

Antibiofilm
Bacterial predator
Liposome
Drug delivery

ABSTRACT

Biofilms increase bacterial resistance to antibiotics, as conventional antibiotic doses are often ineffective at penetrating the biofilm matrix to eliminate bacteria. Recent research has shown that the Gram-negative predator bacterium *Bdellovibrio bacteriovorus* can penetrate Gram-positive bacterial biofilms during its predation phase and benefit from them without direct predation. Here, based on the penetration ability of *B. bacteriovorus*, we constructed antibiotic-loaded liposome-engineered *B. bacteriovorus* as a drug delivery strategy for biofilm-related diseases. As a “living antibiotic,” *B. bacteriovorus* can prey on Gram-negative bacteria, penetrate biofilms, and disrupt their dense structure. During this process, the rapid movement of *B. bacteriovorus* enhances the delivery of antibiotic-loaded liposomes into the biofilm, promoting efficient antibiotic release and improving biofilm eradication. Our findings demonstrate that this engineered living antibiotic strategy significantly improves the control and removal of bacterial biofilms, accelerates the elimination of dental plaque, promotes wound healing, and holds promise as a novel platform for treating biofilm-related infections.

1. Introduction

Bacteria are the culprits in chronic infections such as implant infections, caries, periodontitis, and chronic infection of diabetic wounds, and usually exist in the form of biofilm [1–3]. Antibiotics are the conventional treatment for biofilm-related diseases [4]. Bacteria are susceptible to antibiotics in a planktonic state, but become resistant to conventional doses of antibiotics when they secrete polymeric matrices containing polysaccharides, proteins, DNA, and form structurally stable biofilms [5]. As bacteria biofilms grow thicker (up to 50 μm) during the maturation phase, this significantly reduces the diffusion rate of antibiotics through the extracellular polymeric matrix of biofilm and enhances the resistance of bacteria to antibiotics [5–8]. Consequently, the development of more effective strategies to combat antibiotic resistance in biofilms has become a prominent area of research [9,10].

Bdellovibrio bacteriovorus (*B. bacteriovorus*) is a natural predator that can prey on most gram-negative bacteria and a few Gram-positive bacteria [11,12]. When *B. bacteriovorus* detects the presence of prey, it enters “attack phase”, searching for prey at a very fast speed and attaching

to the surface of prey, secreting hydrolytic enzymes, which help it penetrate the periplasm of prey, and then consumes the prey’s nutrients to replicate, and ultimately cause the lyses and death of prey [13]. *B. bacteriovorus* preys on a variety of Gram-negative bacteria disregarding their existing form (planktonic bacteria or biofilm)[14]. Although its predatory ability on Gram-positive bacteria is limited, which restricts its antibacterial application [15], recent studies have shown that *B. bacteriovorus* still exhibits predatory behaviors like high motility and hydrolytic enzymes secretion when encountering Gram-positive bacteria [16,17]. Even without predation, it can still benefit energetically from Gram-positive bacterial biofilms [18,19]. This suggests that *B. bacteriovorus* possesses the ability to penetrate and disrupt biofilms. In addition, studies have demonstrated the safety and low immunogenicity of *B. bacteriovorus* in animals [20–22], providing a possibility for the development of *B. bacteriovorus* as a new broad-spectrum antibiofilm strategy [23,24].

At present, the combination of synthetic materials and non-pathogenic living microbes has shown bright prospects in the treatment of various diseases [25–28]. Our preliminary study showed that

* Corresponding authors.

E-mail addresses: xz-zhang@whu.edu.cn (X.-Z. Zhang), huangcui@whu.edu.cn (C. Huang).

<https://doi.org/10.1016/j.jconrel.2025.01.075>

Received 31 August 2024; Received in revised form 22 January 2025; Accepted 24 January 2025

Available online 6 February 2025

0168-3659/© 2025 Elsevier B.V. All rights are reserved, including those for text and data mining, AI training, and similar technologies.

after modification with materials, *B. bacteriovorus* exhibited enhanced efficacy in removing biofilms of Gram-negative bacteria [29]. Inspired by this, we developed an antibiotic-encapsulated liposome-modified *B. bacteriovorus* with enhanced drug delivery capability and broad-spectrum antibiofilm characteristics. In this multifunctional system, ampicillin-encapsulated liposomes (ALP) were attached to the surface of *B. bacteriovorus* through a condensation reaction, forming ALP@Bdello (Fig. 1a). *B. bacteriovorus* penetrates the biofilms, preys on Gram-negative bacteria, delivers ALP into the biofilm, and promotes drug release in the process of disrupting the structure of biofilms (Fig. 1b). The synergistic effects of *B. bacteriovorus* and ampicillin in ALP@Bdello could effectively remove both Gram-positive and Gram-negative bacterial biofilm (Fig. 1c). In this paper, we evaluated the efficacy of ALP@Bdello for the removal of dental plaque biofilm, general wound biofilm, and diabetic-infected wound biofilm, and the results showed outstanding drug delivery ability and antibiofilm activity. We expect that this living antibiotic strategy will become a viable approach for treating biofilm-related diseases.

2. Materials and methods

2.1. Materials

L- α -phosphatidylcholine (soybean lecithin) was obtained from J&K Scientific (China), DSPE-PEG2000 and DSPE-PEG2000-NHS were obtained from Shanghai Ponsure Biotech, Inc. Cholesterol, methylene chloride, Ampicillin Sodium, Rhodamine B, glutaraldehyde, and methanol were purchased from Aladdin. Dimethyl sulfoxide (DMSO) was obtained from Leyan (Shanghai, China). Cy5.5-NHS and the ELISA kits for mouse IL-1 β and mouse IFN- γ was purchased from Solarbio (China). SYTO 9 was purchased from Thermo Fisher (USA). Calcein-AM and propidium iodide were procured from Beyotime Biotechnology (China). The nutrient broth, lysogeny broth, brain heart infusion, and agar were obtained from Hopebio Biotechnology (China). Fetal bovine serum (FBS, BDAA0122–500 mL) was provided by Biodragon (Suzhou, China). Penicillin-Streptomycin Solution (100 \times) was obtained from Sperikon Life Science & Biotechnology Co., Ltd. Roswell Park Memorial Institute (RPMI) 1640 medium, trypsin, and 5-diphenyltetrazolium-bromide

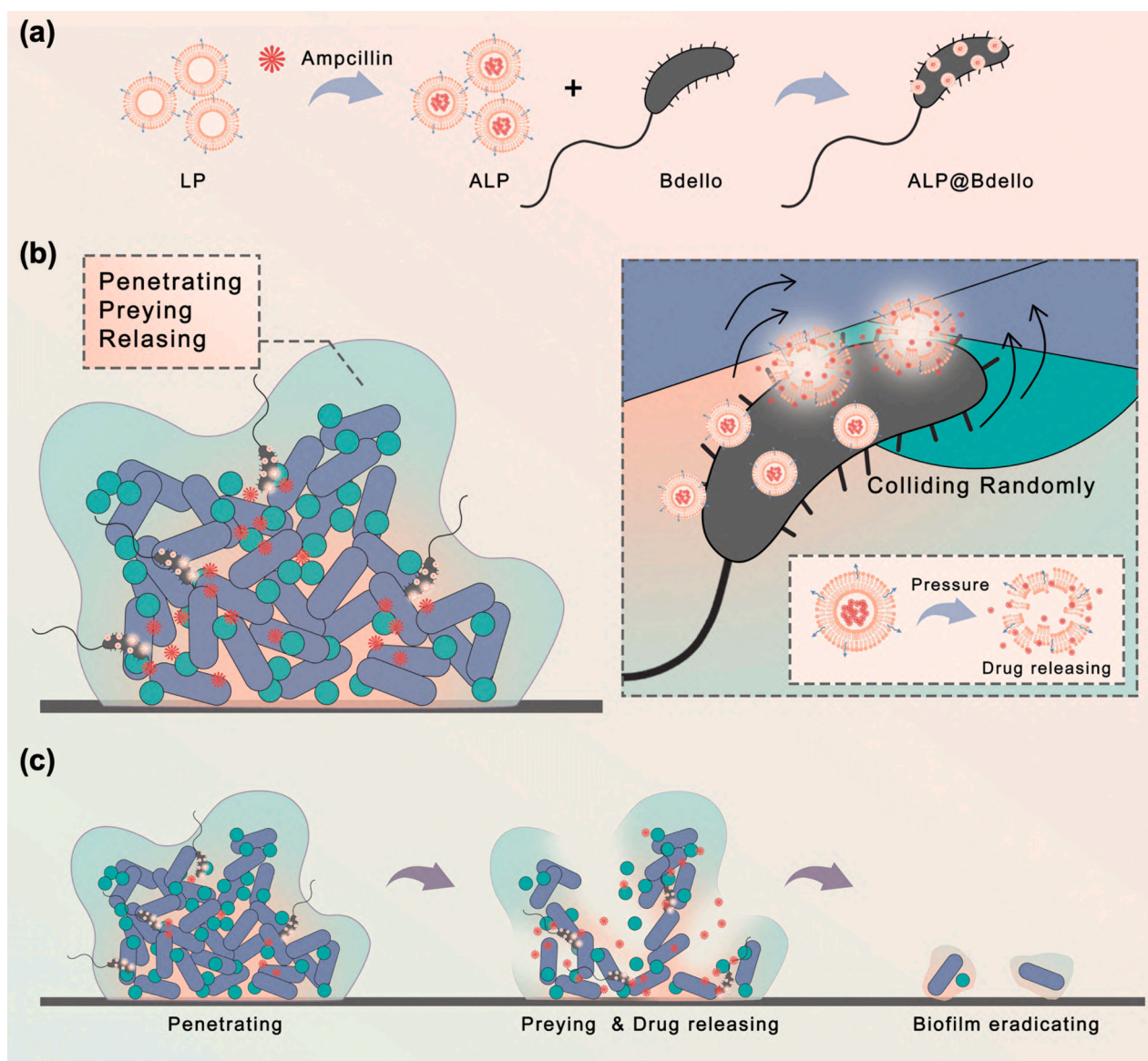


Fig. 1. Schematic illustration of the antibiotic penetration and biofilm eradication process of ALP@Bdello. (a) Preparation steps of ALP@Bdello. (b) ALP@Bdello penetrates the biofilm. During the predation process, random collision of *B. bacteriovorus* promotes liposome rupture and drug release. (c) ALP@Bdello for penetrating and eradicating biofilms.

(MTT) were provided by Invitrogen (USA). glass-bottom dishes (20 mm) and cell culture dishes/plates were procured from NEST Biotechnology Co., Ltd. Confocal petri dishes (35 mm) were obtained from Zhejiang Saining Biotechnology Co., Ltd. Hematoxylin-Eosin (HE) Stain Kit and Masson's Trichrome Stain Kit was purchased from Solarbio (China). DAPI (Cat. No. C3362) was provided by APEX BIO (Houston, USA). Dental plaque stain was purchased from Beikangdengte (China).

2.2. Bacterial strains and culture

Bdellovibrio bacteriovorus HD 100 (ATCC 15356) was obtained from ATCC (U.S.), *Escherichia coli* (ATCC 25922), *Pseudomonas aeruginosa* (ATCC 9022), and *Staphylococcus aureus* (ATCC 6538P) and *Streptococcus mutans* (ATCC 25175) were obtained from Guangdong Microbial Cultural Collection Center (GDMCC).

E. coli and *P. aeruginosa* were cultured with Luria-Bertani (LB) medium, while *S. aureus* was cultured with nutrient broth (NB) medium, and *S. mutans* was cultured with Brain Heart Infusion (BHI) medium.

According to the ATCC Culture Guide, *B. bacteriovorus* was cultured with diluted nutrient broth medium (DNB medium: 2.4 g/L nutrient broth, 1.5 g/L yeast) in 125 mL vented culture flasks. The culture flasks were incubated in a shaking incubator at a constant temperature of 28–30 °C. Then *B. bacteriovorus* propagated by adding *E. coli* as prey. For subsequent experiments, residual prey was filtered and removed using a 0.45 µm Millex pore-size filter (Millipore).

2.3. Preparation and characterization of ALP

To prepare the Liposomes, a thin-film hydration method followed by membrane extrusion was employed. Briefly, 1.0 mg of L- α -phosphatidylcholine, 0.02 mg DSPE-PEG2000-NHS, and 0.25 mg of cholesterol were dissolved using 10.0 mL of methylene chloride in a round-bottom flask and stirred (MS7-S, magnetic stirrer, DLAB Scientific Co., Ltd) for 10 min. Then a phospholipid film was formed through a rotary evaporator under reduced pressure. 1.0 mL of 100 µg/mL solution of Ampicillin Sodium was added into the round bottom flask with phospholipid film for hydration for 1 h. After hydration, liposomes with NHS group loaded with ampicillin (denoted as ALP) were extruded 11 times through 200 nm membranes and purified by ultrafiltration. The amount of unencapsulated ampicillin (denoted as Amp) in the supernatant was determined using HPLC. The encapsulation efficiency was calculated with the formulas: encapsulation efficiency = $(M(\text{feeding}) - M(\text{supernatant})) / M(\text{feeding}) \times 100\%$, and the loading capacity was calculated with the formulas: loading capacity = $(M(\text{feeding}) - M(\text{supernatant})) / M(\text{total}) \times 100\%$. The obtained ALP was stored at 4 °C for further use. Transmission electron microscope (TEM) (JEOL-2100) and scanning electron microscope (SEM) (Zeiss SIGMA) were used to observe the morphology of liposomes. Dynamic light scattering (DLS, Nano-ZS ZEN3600) was used to measure the diameter of ALP.

2.4. Preparation and characterization of ALP@Bdello

B. bacteriovorus (10^7 – 10^8 PFU/mL, 1 mL) was washed three times by centrifugation (7000 rpm, 10 mins) and mixed with ALP (Amp: 5, 10, or 40 µg) at 30 °C for 2 h. The mixed solution was concentrated (7000 rpm, 10 mins) and redispersed in DNB medium to obtain ALP engineered *B. bacteriovorus* (denoted as ALP@Bdello). The unreacted ALP in the supernatant was collected (14,000 rpm, 15 mins) and cracked by methanol, and the Amp in unreacted ALP was detected via ultraviolet-visible spectrophotometry. The final Amp loading of ALP@Bdello was calculated with following formula: $M(\text{loading}) = M(\text{feeding}) - M(\text{supernatant})$. And the grafting rate of ALP on *B. bacteriovorus* was calculated according to the following formula: $\text{Grafting rate} = M(\text{feeding} - \text{supernatant}) / M(\text{feeding}) \times 100\%$. The diameter of *B. bacteriovorus* and ALP@Bdello was measured by dynamic light scattering (DLS, Nano-ZS ZEN3600). The zeta potential of liposome (LP), ALP, *B. bacteriovorus*

alone (Bdello), and ALP@Bdello were detected by DLS. SEM and TEM were used to observe the morphology of ALP@Bdello. To visualize the ALP on Bdello, ALP labeled red with DIL was combined with *B. bacteriovorus*, and the obtained ALP@Bdello were further stained with SYTO 9 (5 µM) and washed with PBS, and then placed in glass-bottom dishes and observed using inverted fluorescence microscopy. To further observe the adhesion and capture of ALP@Bdello on prey, *E. coli* (10^9 CFU/mL, 500 µL) was treated with ALP@Bdello (Amp: ~5 µg/mL, Bdello: 10^7 CFU/mL, 1 mL) in DNB medium for 4 h, then the mixture was centrifuged (7000 rpm, 10 mins), washed with PBS, and fixed by glutaraldehyde, and observed by SEM.

2.5. The vitality of *B. bacteriovorus* after co-cultured with ALP

The double-layer plate method was used to assess the effect of ALP on *B. bacteriovorus* vitality. Since it takes 3–5 days for phage plaques of *B. bacteriovorus* to form on double-layer plates, to ensure better control over the contact time between ALP and *B. bacteriovorus*, it is ALP without NHS groups that was used to incubate with *B. bacteriovorus* (The synthesis method of ALP without the NHS group was essentially the same as that of ALP, but DSPE-PEG2000 was used instead of DSPE-PEG2000-NHS. ALP without the NHS group cannot undergo chemical conjugation with *B. bacteriovorus*). The *B. bacteriovorus* ($\sim 10^7$ PFU/mL, 1 mL) was centrifuged, the precipitate was collected and dispersed with 1 mL of ALP without NHS group (Amp: 0, 1, 2, 4, 8, 16, or 32 µg/mL, respectively). After being incubated for 4 h in a shaker at 30 °C, *B. bacteriovorus* was collected by centrifugation (7000 rpm, 10 mins) and washed with PBS three times. The double-layer plate method was used to quantify the *B. bacteriovorus* that retained predatory viability. The double-layer plate method was based on the literature[30]: Pour ~10 mL of 2 % agar into a petri dish and let it solidify to form the bottom layer. Then add 3–4 mL of semi-solid medium (DNB medium, 0.6 % agar) containing ALP-treated *B. bacteriovorus* (200 µL) and *E. coli* (10^9 CFU/mL, 100 µL) to the dish to form the top layer. Incubate the plate at 30 °C for 3–5 days and determine the activity of *B. bacteriovorus* by counting the number of plaques.

2.6. Drug release behavior of ALP and ALP@Bdello

3 mL of ALP (Amp: ~20 µg/mL) was placed inside a dialysis capsule along with 1 mL of PBS, and 3 mL of ALP@Bdello (Amp: ~20 µg/mL, *B. bacteriovorus*: $\sim 10^7$ PFU/mL) was placed inside a dialysis capsule along with either PBS (1 mL) or *E. coli* ($\sim 10^9$ CFU/mL, 1 mL). The capsules were submerged in 15 mL centrifuge tube containing 8 mL of PBS and placed in a constant temperature shaker (200 rpm, 37 °C). At 0.5, 1, 2, 5, and 8 h of dialysis, 1 mL of liquid was collected from the 8 mL of PBS outside of the dialysis, and 1 mL of fresh drug-free PBS was simultaneously added. The concentrations of Amp that were released from dialysis were measured by ultraviolet-visible spectrophotometry.

2.7. Biocompatibility of ALP@Bdello in vitro

MTT assay: 100 µL NT3T3 cells suspension (10^6 /mL) was seeded in a 96-well plate and cultured in Roswell Park Memorial Institute (RPMI) 1640 medium at 37 °C with 5 % CO₂ and 21 % O₂. Subsequently, different concentrations of ALP@Bdello were resuspended into 1640 medium and added into each well for incubation over 24 h respectively. Then 10 µL of MTT solution was added, 4 h later, the supernatant was removed, 150 µL DMSO was added to dissolve formazan in cells, and the mixture's absorbance was measured at 570 nm with a microplate reader.

Live/dead staining: NT3T3 cells were seeded into 6-well plates and cultured for 24 h at 37 °C. Then the cells were co-incubated with *B. bacteriovorus* ($\sim 10^7$ PFU/mL, 1 mL), ALP@Bdello (Amp: 16 µg/mL, *B. bacteriovorus*: $\sim 10^7$ PFU/mL) for 12 h. After that, the cells were incubated with Calcein-AM (2 µM) and PI solutions (5 µM) for 30 min and observed by fluorescence inverted microscope and counted by

Image J. (Calcein-AM: Ex = 490 nm, Em = 515 nm; PI: Ex = 545 nm, Em = 617 nm).

2.8. Biocompatibility of ALP@Bdello in vivo

Twelve healthy female KM mice (4 weeks old) were treated with PBS, *B. bacteriovorus* ($\sim 10^7$ PFU/mL, 1 mL), ALP@Bdello (Amp: 16 $\mu\text{g}/\text{mL}$, *B. bacteriovorus*: $\sim 10^7$ PFU/mL) (orally, once a week). At eight weeks after treatment, mouse blood was collected for routine blood test, serum was collected for measurement of the levels of IL-1 β and INF- γ secretion in mouse serum by ELISA kits, and vital organs were collected for histological staining to observe the inflammation in vital organs.

2.9. Antibacterial effects of ALP@Bdello

First, the antibacterial ability of ampicillin on *E. coli*, *P. aeruginosa*, *S. aureus*, and *S. mutans* was measured. Different concentrations of ampicillin (Amp) (0, 1, 2, 4, 8, 16, or 32 $\mu\text{g}/\text{mL}$) were added to the bacterial suspension. After 12 h, the OD value (600 nm) of the bacteria was detected using a microplate reader. We chose ampicillin concentrations that provided approximately 50–70 % inhibitory effect for subsequent experiments, which were 8, 16, 1, 4 $\mu\text{g}/\text{mL}$ for *E. coli*, *P. aeruginosa*, *S. aureus*, and *S. mutans* respectively. Then we added the corresponding concentrations of Amp and ALP into the bacteria solution of *E. coli* (Amp or Amp in ALP: 8 $\mu\text{g}/\text{mL}$), *P. aeruginosa* (Amp or Amp in ALP: 16 $\mu\text{g}/\text{mL}$), *S. aureus* (Amp or Amp in ALP: 1 $\mu\text{g}/\text{mL}$), and *S. mutans* (Amp or Amp in ALP: 4 $\mu\text{g}/\text{mL}$), and detected the OD value (600 nm) of the bacteria using a microplate reader 12 h later. In the subsequent antibacterial and antibiofilm experiments, ALP@Bdello was diluted to achieve the required ampicillin working concentration.

In the liquid-phase antibacterial experiments, *E. coli* ($\sim 10^7$ CFU/mL, 1 mL) was concentrated and treated overnight with 1 mL of PBS, Bdello ($\sim 10^7$ PFU/mL), ALP (~ 8 $\mu\text{g}/\text{mL}$ of Amp), ALP + Bdello (~ 8 $\mu\text{g}/\text{mL}$ of Amp, $\sim 10^7$ PFU/mL of *B. bacteriovorus*), or ALP@Bdello (~ 8 $\mu\text{g}/\text{mL}$ of Amp, $\sim 10^7$ PFU/mL of *B. bacteriovorus*) respectively. The same treatments were performed on *P. aeruginosa*, *S. aureus*, and *S. mutans*, and the Amp concentration in the ALP, ALP + Bdello, and ALP@Bdello groups being 16, 1, 4 $\mu\text{g}/\text{mL}$ for *P. aeruginosa*, *S. aureus*, and *S. mutans*, respectively. After 12 h of incubation, the surviving bacteria were quantified using the flat plate coating method, and were observed by SEM (treated-bacterial were fixed with 2.5 % glutaraldehyde and dehydrated through an ethanol gradient).

2.10. Biofilm construction

E. coli, *P. aeruginosa*, and *S. aureus* ($\sim 10^7$ CFU/mL, 1 mL) were inoculated into confocal dishes, respectively. The medium was changed every other day until the established biofilm could be observed by the naked eyes (about 3–5 days). *S. mutans* ($\sim 10^8$ CFU/mL, 20 μL) was inoculated into 1 mL of BHI medium with sucrose (17 g/L) in confocal dishes. After 12 h, the biofilm was formed on the bottom of the confocal dish. The biofilm was labeled with SYTO 9 for 15 mins and observed by CLSM.

2.11. The drug delivery ability of RLP@Bdello

To better observe the position of the drug in the biofilm, we loaded Rhodamine B in liposomes. To prepare Rhodamine B-loaded liposomes (RLP), a 0.02 mg/mL solution of RhB solution was used to replace the PBS in the hydration process. Rhodamine B loaded in RLP was then lysis by methanol and detected by fluor spectrophotometer. RLP@Bdello was synthesized similarly to ALP@Bdello, but using RLP instead of ALP.

S. aureus biofilms were constructed in the confocal dishes and labeled with SYTO 9. After washing with PBS, the biofilms were treated with 1 mL free RhB (5 $\mu\text{g}/\text{mL}$), RLP (5 $\mu\text{g}/\text{mL}$ of RhB), or RLP + Bdello (5 $\mu\text{g}/\text{mL}$ of RhB, $\sim 10^7$ PFU/mL of *B. bacteriovorus*), or RLP@Bdello (5 $\mu\text{g}/\text{mL}$

of RhB, $\sim 10^7$ PFU/mL of *B. bacteriovorus*), respectively. The biofilms were incubated for an additional 2 h at 30 °C, and the position of RhB in the biofilm was observed by CLSM. (SYTO 9: Ex = 488 nm, Em = 520 nm; RhB: Ex = 540 nm, Em = 625 nm).

2.12. Antibiofilm effects of ALP@Bdello

First, *E. coli*, *P. aeruginosa*, *S. aureus*, and *S. mutans* biofilms was cultured in confocal dishes. Then, the biofilm was treated separately with different materials: 1 mL of PBS, Bdello ($\sim 10^7$ PFU/mL), ALP (8 $\mu\text{g}/\text{mL}$ of Amp), ALP + Bdello (8 $\mu\text{g}/\text{mL}$ of Amp, $\sim 10^7$ PFU/mL of *B. bacteriovorus*), or ALP@Bdello (8 $\mu\text{g}/\text{mL}$ of Amp, $\sim 10^7$ PFU/mL of *B. bacteriovorus*) was added in the *E. coli* biofilm. The same treatments were performed on the biofilm of *P. aeruginosa*, *S. aureus*, or *S. mutans*, and the concentration of ampicillin in the ALP, ALP + Bdello, and ALP@Bdello groups were 16, 1, 4 $\mu\text{g}/\text{mL}$ for *P. aeruginosa*, *S. aureus*, and *S. mutans*, respectively. After 12 h of co-incubation, the residual biofilm was labeled with SYTO 9 and observed by CLSM. The residual area of biofilm was measured by imageJ. (SYTO 9: Ex = 488 nm, Em = 520 nm).

2.13. Antibiofilm effects of ALP@Bdello on ex vivo human teeth

Intact caries-free human third molars were collected from clinical patients, and the teeth were cleaned and placed in thymol solution and stored at 4 °C. Caries-free third molars were cut into slices (5 × 5 × 2 mm, L × W × H). After UV sterilization for 2 h, 15 dental slices were placed in 24-well plates and submerged in 1 mL sucrose-containing BHI medium with *S. mutans* (10^5 CFU/mL) for 12 h to construct *S. mutans* biofilm on the dental slices. The dental slices with *S. mutans* biofilm were washed with PBS and treated with 1 mL of PBS, Bdello ($\sim 10^7$ PFU/mL), ALP (4 $\mu\text{g}/\text{mL}$ of Amp), ALP + Bdello (4 $\mu\text{g}/\text{mL}$ of Amp, $\sim 10^7$ PFU/mL of *B. bacteriovorus*), or ALP@Bdello (4 $\mu\text{g}/\text{mL}$ of Amp, $\sim 10^7$ PFU/mL of *B. bacteriovorus*), respectively. After 12 h of treatment, the supernatant was removed and the dental slices were washed with PBS and fixed with 2.5 % glutaraldehyde, then dehydrated by ethanol gradient and observed by SEM.

Five caries-free third molars with oral microbial were placed in 24-well plates and submerged in 1 mL sucrose-containing BHI medium for 12 h to construct *S. mutans* mixed biofilm on the teeth directly. The teeth covered with oral biofilm were stained with dental plaque stain and recorded with a digital camera, then treated with 1 mL of PBS, Bdello (10^7 PFU/mL), ALP (16 $\mu\text{g}/\text{mL}$ of Amp), ALP + Bdello (16 $\mu\text{g}/\text{mL}$ of Amp, $\sim 10^7$ PFU/mL of *B. bacteriovorus*), or ALP@Bdello (16 $\mu\text{g}/\text{mL}$ of Amp, $\sim 10^7$ PFU/mL of *B. bacteriovorus*), respectively. After 12 h of treatment, the supernatant was removed and the teeth were stained with dental plaque stain and recorded with a digital camera.

2.14. Antibacterial efficiency of ALP@Bdello in vivo

Animal experiments were approved by the School and Hospital of Stomatology of Wuhan University Medical Ethics Committee (Approval number: 2019LUNSHENA40). In order to observe the predatory ability of ALP@Bdello in vivo, a 5 mm skin wound model was created on the backs of KM mice ($n = 3$), and the wound was infected with bioluminescent *E. coli* ($\sim 10^8$ CFU/mL, 100 μL). Then the wounds were treated with 100 μL of PBS, Bdello ($\sim 10^7$ PFU/mL of *Bdellovibrio*), ALP (8 $\mu\text{g}/\text{mL}$ of Amp), ALP + Bdello (8 $\mu\text{g}/\text{mL}$ of Amp, $\sim 10^7$ PFU/mL of *B. bacteriovorus*), or ALP@Bdello (8 $\mu\text{g}/\text{mL}$ of Amp, $\sim 10^7$ PFU/mL of *B. bacteriovorus*) three times over a 12-h period. The bioluminescent *E. coli* adhering on wounds were imaged using an IVIS system at different times.

2.15. Skin wound model

Mouse skin wound model: Twelve healthy female KM mice (4 weeks old) were used to construct the skin wound (5 mm) on their backs. The

wound was then infected with a mixture of 20 μL of *E. coli* bacterial solution ($\sim 10^8$ CFU/mL) and 20 μL of *S. aureus* solution ($\sim 10^8$ CFU/mL). Mice were divided randomly into 4 groups, and the wounds were treated with 50 μL of PBS, Bdello ($\sim 10^7$ PFU/mL *B. Bdellovibrio*), ALP (8 $\mu\text{g}/\text{mL}$ Amp), ALP + Bdello (8 $\mu\text{g}/\text{mL}$ Amp, $\sim 10^7$ PFU/mL *B. Bdellovibrio*), or ALP@Bdello (8 $\mu\text{g}/\text{mL}$ Amp, $\sim 10^7$ PFU/mL *B. Bdellovibrio*) three times a day, for one week. Wound healing was captured using a digital camera on days 1, 3, 5 and 7, and measured and analyzed by Image J. And the Blood samples were collected on day 2 and detected by Blood Biochemistry Analy7zer (MNCHIP POINTCARE) and

Auto Hematology Analyzer (MC-6200VET).

2.16. Diabetic mice skin wound model

STZ-induced diabetic mice were established according to the literature [31]. A circular full-thickness wound (diameter: 8 mm) was produced on the back of diabetic mice, and infected with 20 μL of *E. coli* solution ($\sim 10^8$ CFU/mL) and 20 μL of *S. aureus* solution ($\sim 10^8$ CFU/mL). The mice were then randomly divided into 4 groups ($n = 6$) and treated with 50 μL of PBS, *Bdellovibrio* ($\sim 10^7$ PFU/mL), ALP (8 $\mu\text{g}/\text{mL}$

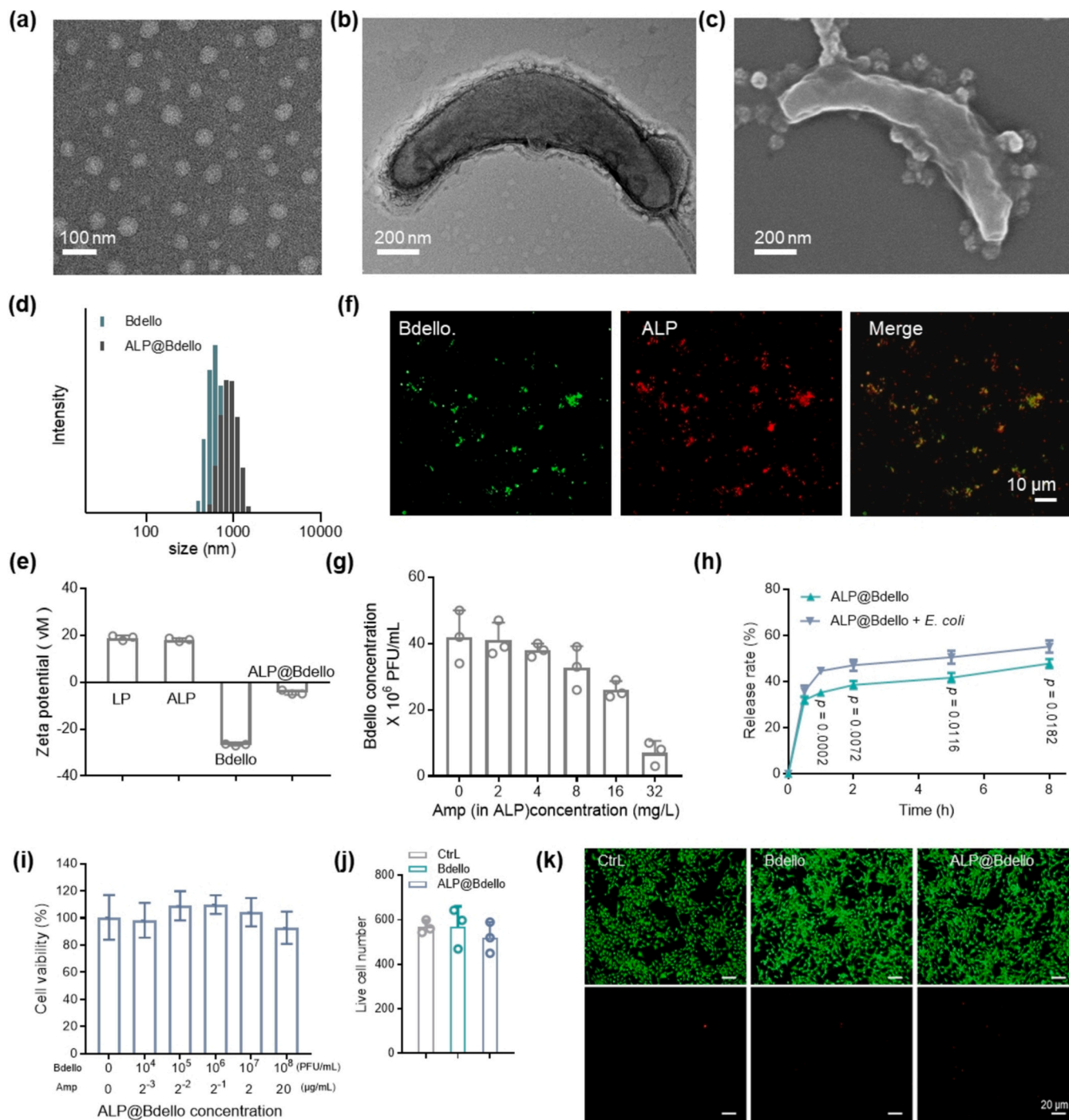


Fig. 2. Characterization of ALP@Bdello. (a) TEM image of ALP. (b) TEM and (c) SEM images of ALP@Bdello. (d) Size of Bdello and ALP@Bdello. (e) Zeta potential of LP, ALP, Bdello, and ALP@Bdello. (f) Fluorescence images of ALP@Bdello (ALP labeled with DiI, and *B. bacteriovorus* labeled with SYTO 9). (g) Effects of different concentrations of Amp in ALP on *B. bacteriovorus*. (h) Release curve of Amp in ALP@Bdello with or without prey (*E. coli*). (i) Effect of different concentrations of ALP@Bdello on NT3T3 cells. (j) Live-dead statistical analysis and (k) staining images of NT3T3 cells after Bdello or ALP@Bdello treatment.

Amp), ALP + Bdello (8 µg/mL Amp, $\sim 10^7$ PFU/mL *B. Bdellovibrio*), or ALP@Bdello (8 µg/mL of Amp, $\sim 10^7$ PFU/mL of *B. bacteriovorus*) three times a day for 14 days, respectively. To observe the wound healing process, wounds were measured using a digital caliper and photographed at days 0, 3, 7, and 14. On day 14, the mice were sacrificed, and the wound tissues were collected. The biofilm residues on wound tissues and expression of inflammatory factors were observed by SEM and histological staining.

2.17. Statistical analysis

The data in this study are presented as mean \pm SD. Data were analyzed using GraphPad Prism 7 and SPSS 17.0 software. To assess statistical significance between two groups, a two-tailed unpaired Student's *t*-test was used, while one-way ANOVA was employed for comparisons among multiple groups.

3. Results and discussion

3.1. Synthesis and characterizations of ALP@Bdello

Ampicillin@liposome-NHS (ALP) was synthesized according to the previous research [32]. The obtained ALP exhibited a diameter of approximately 50–100 nm, with a polydispersity index (PDI) of 0.18, as observed in the TEM image (Fig. 2a), the SEM image (Fig. S1a) and the dynamic light scattering (DLS) analysis (Fig. S1b). The encapsulation efficiency of Ampicillin (Amp) within ALP was determined using HPLC and was estimated to be approximately 23 %, according to the standard curve (Fig. S2). The loading capacity of Amp within ALP, determined after lyophilization, was calculated to be approximately 2 %. As measured by dialysis, the release of ampicillin in ALP at 2 h was about 50 % (Fig. S3).

B. bacteriovorus was fed with *Escherichia. Coli* (*E. coli*) and purified as described in the literature [33]. ALP engineered *B. bacteriovorus* (ALP@Bdello) was obtained through a condensation reaction between NHS (on the ALP) and amines (on the surface of *B. bacteriovorus*). After the reaction, the liquid was centrifuged to obtain ALP@Bdello, and the remaining ALP in the supernatant was collected and ruptured. The grafting rate of ALP@Bdello was measured to be approximately 60–70 % when the feeding amount of Amp in ALP is 5–40 µg (Fig. S4, S5). TEM (Fig. 2b) and SEM (Fig. 2c) images of ALP@Bdello confirmed the successful attachment of ALP to the surface of *B. bacteriovorus*. The size of ALP@Bdello was slightly increased compared with *B. bacteriovorus* alone (Fig. 2d), and the zeta potential (Fig. 2e) of ALP, *B. bacteriovorus* (referred to as Bdello), and ALP@Bdello changed obviously during the synthesis process. Subsequently, ALP was labeled with DIL (red) and attached to the surface of *B. bacteriovorus*, which was labeled SYTO 9 (green). Fluorescence microscopy result (Fig. 2f) demonstrated overlapping red and green fluorescence, confirming successful attachment of ALP to *B. bacteriovorus*.

According to the literature, *B. bacteriovorus* completes its lifecycle of attaching, drilling, predation, replication, and lysing of the host within four hours [11,15]. Given the potential impact of Amp on *B. bacteriovorus* activity, we detected its performance after exposure to varying concentrations of ALP using the double-layer plate method [30]. As depicted in the results (Fig. 2g), even at a loading concentration of 16 mg/L of Amp in ALP, *B. bacteriovorus* maintained a good predation ability on Gram-negative bacteria after a 4-h incubation period. However, at a loading concentration of 32 mg/L of Amp, the activity of *B. bacteriovorus* was significantly compromised. In addition, we observed the predatory effect of ALP@Bdello on prey by SEM. The image (Fig. S6) showed that ALP@Bdello, which was in the adhesion stage, encountered and attached to the surface of prey (*E. coli*), indicating that the predatory ability of *B. bacteriovorus* is not affected by ALP backpack.

Previous studies have demonstrated that *B. bacteriovorus* exhibits motility, capable of rotational movement at speeds of up to 160 µm/s

during the attack phase [34–36]. Our own research has further highlighted the mechanical force generated by *B. bacteriovorus* upon collision with its hosts [29]. Given that the release of Amp from ALP@Bdello may be influenced by these mechanical forces during *B. bacteriovorus* movement, we investigated the release behavior of Amp from ALP@Bdello in the presence or absence of *E. coli*. As shown in Fig. 2h, the release rate of Amp from the ALP@Bdello group was significantly lower than that from the ALP@Bdello + *E. coli* group. This difference indicates that in the presence of *E. coli*, the active and random movements of *B. bacteriovorus* lead to increased collisions, thereby enhancing the rupture of attached ALP and accelerating Amp release.

3.2. The biocompatibility of ALP@Bdello

Liposomes have been widely used in drug delivery for various diseases due to their unique physiological functions and reduced systemic toxicity [37–39]. *B. bacteriovorus* also shows low toxicity both in vitro and in vivo [20–22]. To verify the biosafety of ALP@Bdello in vitro, we treated NT3T3 cells with different concentrations of ALP@Bdello and conducted an MTT assay. The results (Fig. 2i) showed that even at a concentration of 10^7 PFU/mL, ALP@Bdello exhibited negligible adverse effects on cell viability. Additionally, microscopic examination revealed minimal cell death in the ALP@Bdello-treated group (Fig. 2j, k). To further assess the biosafety of ALP@Bdello in vivo, we administered ALP@Bdello treatment to mice and evaluated the safety and potential immune response of introducing *B. bacteriovorus* or ALP@Bdello to the host through blood routine tests, inflammatory cytokine levels, and histological staining of major organs. The results (Fig. S7, S8) show that, at the 8th week after introduction into the host system, neither *B. bacteriovorus* nor ALP@Bdello caused significant toxicity or triggered a notable immune response. Based on our experimental results, the immune response trigger by ALP@Bdello is negligible, which can be attributed primarily to the favorable biosafety of *B. bacteriovorus*, as well as the high safety of liposomes and antibiotics, which are widely used in the biopharmaceutical field. For humans, engineered *B. bacteriovorus* offer good biosafety and low immune response, which means that during the process of controlling biofilm infections, a safer and more stable microbial environment can be maintained in the host. The mild nature of engineered *B. bacteriovorus* and its low immunogenicity result in minimal stimulation to the host's immune system, effectively avoiding excessive immune responses within the host, and the risk of severe side effects during long-term use is reduced. This mild characteristic makes it potentially suitable for individuals with various constitutions, including those with weakened immune functions or those in need of long-term care. This gives engineered *B. bacteriovorus* the potential to be used as a long-term health intervention, making it a relatively safe and enduring option.

3.3. In vitro antibacterial activity of ALP@Bdello

Infectious bacterial diseases pose significant threats to human health, particularly affecting immunocompromised patients, sometimes leading to fatalities [40,41]. Currently, antibiotics are widely utilized to manage bacterial biofilm-related diseases [42]. However, the long-term use of antibiotics has spurred the rise of the emergence of drug-resistant bacteria [43], a trend escalating rapidly in recent years [44]. Therefore, addressing bacterial drug resistance and developing novel therapeutics are of paramount importance. In this part, we investigated the predatory capacity of *B. bacteriovorus* against Gram-negative bacteria, revealing a positive correlation between its predation capability and concentration (Fig. 3a), achieving 50–60 % at 10^7 PFU/mL.

Next, we assessed the inhibitory effects of Amp on four common bacteria, observing inhibition rates ranging from 50 to 70 % at an Amp concentration of 8 mg/L for *E. coli*, 16 mg/L for *P. aeruginosa*, 1 mg/L for *S. aureus*, and 4 mg/L for *S. mutans* (Fig. S9). Then we compared the antibacterial effects of Amp and ALP (above concentration) in treating

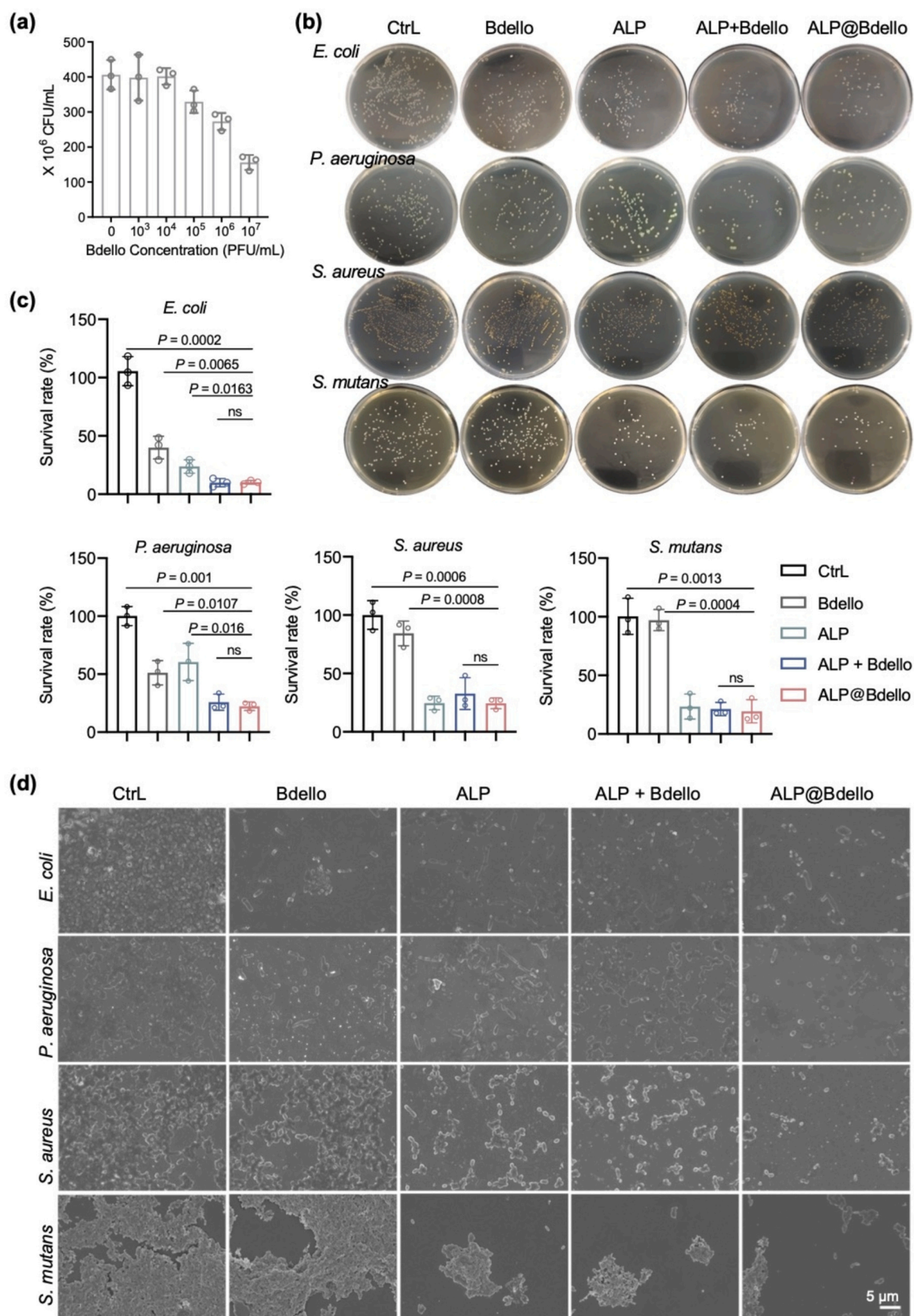


Fig. 3. Antibacterial effects of ALP@Bdello. (a) Viability of *E. coli* treated with different concentrations of *B. bacteriovorus*. (b) Digital photographs and (c) statistical analysis of the bacterial colony of *E. coli*, *P. aeruginosa*, *S. aureus*, and *S. mutans* after treatment with PBS, Bdello, ALP, ALP + Bdello, or ALP@Bdello. (d) SEM images of *E. coli*, *P. aeruginosa*, *S. aureus*, and *S. mutans* after treatment with PBS, Bdello, ALP, ALP + Bdello, or ALP@Bdello, respectively.

bacteria overnight, and the results (Fig. S10) showed no significant differences. Therefore, we focused on comparing the difference between ALP and ALP@Bdello in the following experiments. To explore the synergistic effect between ALP and Bdello, we used *B. bacteriovorus* at 1×10^7 PFU/mL and the aforementioned Amp concentrations in the ALP@Bdello in the subsequent antibacterial and antibiofilm experiments.

Next, we evaluated the antibacterial effects of PBS, Bdello, ALP, ALP + Bdello (ALP without NHS groups, mixed with *B. bacteriovorus*), and ALP@Bdello on these four pathogens in the planktonic phase. As the results showed (Fig. 3b, c), for Gram-negative bacteria, Bdello exhibited approximately 50–60 % inhibition, ALP exhibited approximately 70 % inhibition for *E. coli* and 40 % for *P. aeruginosa*. The inhibition effect of the ALP + Bdello and ALP@Bdello group was around 80–90 % for *E. coli*, and was around 70–80 % for *P. aeruginosa*. For Gram-positive bacterium, which cannot be preyed by *B. bacteriovorus* there was no significant difference in inhibition among ALP, ALP + Bdello, and ALP@Bdello group, all showing inhibition of *S. aureus* by about 70–75 % and *S. mutans* by about 75–80 % respectively. SEM images of bacteria shown in Fig. 3d and Fig. S11 (magnification) also showed a similar phenomenon after being treated with different materials. These results confirm that *B. bacteriovorus* can prey on *E. coli* and *P. aeruginosa*, working like antibiotics. Moreover, both ALP + Bdello and ALP@Bdello exhibited stronger inhibitory activity against planktonic bacteria compared to ALP or Bdello alone, regardless of whether ALP was attached to *B. bacteriovorus* or not.

3.4. The penetration of RLP@Bdello in biofilm

In the 3.3 antibacterial experiment, we observed the superimposed antibacterial effect of the combination of antibiotic and *B. bacteriovorus* against pathogenic bacteria. However, bacteria usually exist in the form of biofilm, which are composed of bacteria and their extracellular polymeric substances (EPS) includes DNA, polysaccharides, lipids, proteins, and other components, preventing drug penetration and enhancing bacterial resistance to antibiotics [45,46]. There is currently evidence that *B. bacteriovorus* can attack prey, whether the prey is in a planktonic state or biofilm state [14]. When *B. bacteriovorus* detects the presence of prey, it enters “attack phase”, in which *B. bacteriovorus* can move rapidly, attach to the surface of the prey, and penetrate the surrounding matrix, then consuming the prey’s nutrients for growth and replication, ultimately lysing and killing the prey. During predation, *B. bacteriovorus* moves at a high speed, reaching up to 160 $\mu\text{m/s}$ [47]. The research has found that *B. bacteriovorus* is capable of preying on bacteria with thick polysaccharide capsules [48], and can hunt in highly viscous environments [49], also exhibiting gliding motility [50]. These features explain how *B. bacteriovorus* penetrates into biofilm through movement. In addition, *B. bacteriovorus* has a powerful hydrolytic arsenal, including 150 proteases and peptidases, 10 sucrases, 20 deoxyribonucleases, 9 ribonuclease families, and 5 lipases, which is used in *B. bacteriovorus*’s invasion and degradation of extracellular polymeric substances [51]. The attack behaviors exhibited by *B. bacteriovorus* such as high motility and secretion of hydrolytic enzymes may facilitate its penetration within bacteria biofilm and enhance its drug delivery capabilities.

Therefore, we investigated the capability of *B. bacteriovorus* to enhance drug penetration in biofilms. To better observe the penetration of the drug in the biofilm, rhodamine B (RhB) was loaded in liposomes (referred to as RLP) which were packaged by *B. bacteriovorus* to construct RLP@Bdello. Based on the standard curve of RhB (Fig. S12), the concentration of RhB in the RLP group and RLP@Bdello group was measured. Next, *S. aureus* biofilms were constructed and labeled with SYTO 9, and free RhB, RLP, RLP + Bdello, and RLP@Bdello were applied to treat the biofilms respectively. After two hours, the spatial position of rhodamine (red) within the biofilm (green) was observed using a laser confocal scanning microscope. As shown in Fig. 4a, the *S. aureus* biofilm

had a thickness of approximately 60 μm . By observing the cross-section structure of the biofilm, it reveals that such a thickness of biofilms hinders the penetration of RhB or RLP into the biofilm, resulting in the drug being mainly retained at the biofilm surface. Comparing the RLP + Bdello group to the RLP@Bdello group, it was evident that RhB in the RLP@Bdello group penetrated deeper into the biofilm. These results demonstrate that anchoring liposomes onto the *B. bacteriovorus* surface as a backpack enhances drug delivery efficiency within biofilms.

The possible mechanism of RLP@Bdello promoting drug penetration is that when RLP@Bdello interacts with the biofilm, it enters the “attack phase”, exhibiting attack behaviors such as high motility, secretion of hydrolytic enzymes in biofilms. This enables RLP@Bdello to penetrate the biofilm, degrade the extracellular matrix, and thereby enhance drug penetration. In contrast, other drugs such as free RhB and RLP show poor penetration, primarily because the extracellular polymeric substances matrix of the biofilm can block or hinder the penetration of drugs such as antibiotic, protecting the bacteria within the biofilm from antibiotic attacks [52]. This is also why biofilms have a significantly higher antibiotic resistance [5,53].

3.5. The antibiofilm activity of ALP@Bdello in vitro

Next, we evaluated the efficacy of ALP@Bdello in removing biofilms formed by various pathogenic bacteria. Biofilms of *E. coli*, *P. aeruginosa*, *S. aureus*, or *S. mutans* were constructed and treated with PBS, Bdello, ALP, ALP + Bdello, or ALP@Bdello for 12 h respectively. As shown in Fig. 4b and c, in the Bdello group, *B. bacteriovorus* alone removed approximately 70–80 % Gram-negative bacterial biofilm. Additionally, *B. bacteriovorus* also exerts some degree of disruption to Gram-positive bacterial biofilms (20–40 %). In the ALP group, the inhibitory rate of ALP on bacterial biofilm (inhibitory rate: 30–50 %) was significantly lower than that on liquid phase bacteria (inhibitory rate: 40–80 %) (Fig. 3c, 4c). This is related to the inability of the drug to penetrate biofilm structure. For the antibacterial effect on free-floating bacteria, the ALP + Bdello group shows results similar to those of the ALP@Bdello group (Fig. 3c). However, for the antibiofilm effect, compared to the ALP + Bdello group, the ALP@Bdello treatment (with an inhibition rate of 90–95 %) demonstrates higher removal efficiency against both Gram-negative and Gram-positive bacterial biofilms. When considering the results against planktonic bacteria (Fig. 3c) and the drug-delivery capabilities of *B. bacteriovorus* (Fig. 4a), it can be inferred that anchoring ALP onto the surface of *B. bacteriovorus* cells, rather than a simple mixture of these two (ALP + Bdello group), appears to achieve the most effective biofilm removal.

From the previous results, it is evident that the *B. bacteriovorus* with ALP backpack retains a certain level of activity (Fig. 2g). The *B. bacteriovorus* with ALP backpack can penetrate the biofilm, facilitating drug delivery and enhancing the biofilm clearance efficiency (Fig. 4c). Combined the antibiofilm results, it is suggested that ALP@Bdello enters “attack phase” when encountering the biofilm. It exhibits attack phase including high motility and hydrolytic enzyme secretion, and preys on Gram-negative bacteria. During this process, the drug within in the backpack is disrupted and released. Interestingly, even though the *B. bacteriovorus* cannot prey on Gram-positive bacteria, *B. bacteriovorus* alone can still cause some degree of disruption to Gram-positive bacterial biofilms (removal rate around 20–40 %). This may be related to the behavioral changes in *B. bacteriovorus* upon contact with Gram-positive bacteria. Studies have shown that when *B. bacteriovorus* is co-cultured with biofilms of Gram-positive bacteria, there is a significant increase in the expression of genes related to flagella biosynthesis, gliding motility, chemotaxis, and protein hydrolysis [54]; and displays predatory behaviors such as exhibiting high motility and secreting hydrolytic enzymes [16,55]. Im H. et al. demonstrated that *B. bacteriovorus* can acquire amino acids from non-prey biofilms and utilize these amino acids to synthesize and secrete proteases, while also increasing ATP reserves and predatory activity, thereby deriving significant benefits

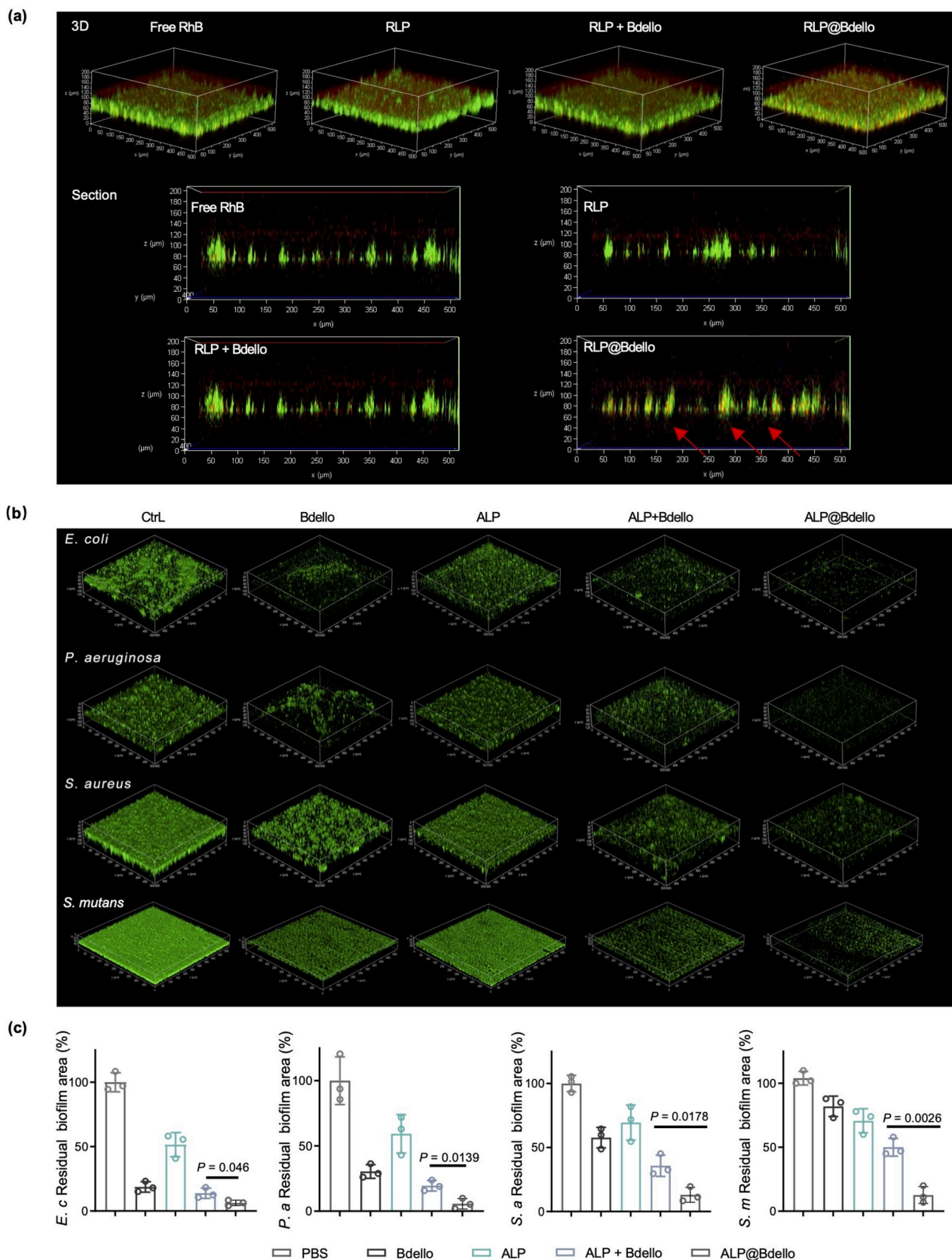


Fig. 4. Biofilm penetration and antibiofilm effects of ALP@Bdello. (a) Spatial distribution of RhB in the biofilm after treatment with free RhB, RLP, RLP + Bdello, or RLP@Bdello for 2 h. (b) Three-dimensional reconstructed fluorescence images and (c) statistical analysis of residual biofilm of *E. coli*, *P. aeruginosa*, *S. aureus*, and *S. mutants* after treatment with PBS, Bdello, ALP, ALP + Bdello, or ALP@Bdello.

from biofilms of Gram-positive bacteria that have not been preyed upon [18]. It is currently generally believed that *B. bacteriovorus* also enters the “attack phase” when co-cultured with Gram-positive bacterial biofilms. Even if *B. bacteriovorus* does not proceed to the next step of predation, its high motility and hydrolytic enzymes secretion will still lead to the degradation of the Gram-positive bacteria biofilm matrix. This content explains how ALP@Bdello can penetrate the biofilms of Gram-positive bacteria.

3.6. The antibiofilm effect of ALP@Bdello on the tooth

In previous studies [29], we evaluated the therapeutic efficacy of engineered *B. bacteriovorus* for periodontitis with Gram-negative bacteria as the main pathogen. However, this strategy isn't applicable in dental caries where the main pathogenic factor is Gram-positive bacterial *S. mutans*. Therefore, we evaluated the efficacy of the ALP@Bdello system in removing *S. mutans* biofilm formed on the tooth. The *S. mutans* biofilms were cultured on tooth slices and treated overnight with PBS, Bdello, ALP, ALP + Bdello, or ALP@Bdello, respectively. As shown in Fig. 5a, ALP@Bdello treatment resulted in the least residual biofilm on the tooth slices compared to the other groups. In addition, patient teeth were collected and cultured in BHI suspension. After the plaque biofilm sufficiently covered the tooth surface, the teeth were treated with PBS, Bdello, ALP, ALP + Bdello, or ALP@Bdello, respectively. By staining the biofilm on the tooth surface with clinical plaque stains, we observed that ALP@Bdello was more effective in removing biofilm from the tooth compared to the other treatment (Fig. 5b).

3.7. In vivo anti-biofilm effect of ALP@Bdello

Next, we constructed a mouse skin wound model to evaluate the in vivo antibacterial efficacy of ALP@Bdello. The wounds were inoculated with biofluorescent *E. coli*, then treated with PBS, Bdello, ALP, ALP + Bdello, or ALP@Bdello, and observed the *E. coli* colonization in the wounds. As shown in Fig. 5c, *E. coli* was almost eliminated in the ALP@Bdello group after 12 h, while it remained abundant in the other groups.

Besides, an infected wound model on healthy mice was developed and treated with PBS, Bdello, ALP, ALP + Bdello, or ALP@Bdello. The wound healing process was recorded on days 1, 3, 5, and 7, and wound areas were quantified by Image J. The results (Fig. 5d-f) revealed that the unhealed wound area in the ALP@Bdello group was 17.4 %, while it was 25.2 %, 27.8 % and 23.4 % in the Bdello, ALP and ALP + Bdello groups, respectively. These results indicate that ALP@Bdello exhibits effective antibiofilm properties on skin wounds in vivo. Meanwhile, blood biochemistry and blood routine tests (Fig. 5g) indicated that ALP@Bdello had no significant adverse effect on liver and kidney function or on blood cells. Taken together, these results suggest that ALP@Bdello exhibits negligible toxicity in vivo and can effectively inhibit the growth of *E. coli* on skin wound surfaces.

3.8. Therapeutic effects of ALP@Bdello on diabetic wound healing

The healing process of diabetic wounds is often prolonged due to the immoderate inflammatory reaction and reduced angiogenesis capacity, combined with mixed infections of multiple bacteria such as *S. aureus* with *E. coli* [56,57], which increases the difficulty of clinical management. Such a complex in vivo microenvironment may affect the local drug delivery and biofilm efficacy of ALP@Bdello. Therefore, we established a diabetic mouse model with multiple bacteria-infected wounds to evaluate the properties of ALP@Bdello under these complex conditions. Wounds were treated with PBS, Bdello, ALP, ALP + Bdello, or ALP@Bdello three times a day for two weeks (Fig. 6a). The skin wounds were recorded on days 1, 3, 7, 10, and 14, and the areas of wounds were quantified by Image J. As shown in Fig. 6b, the ALP@Bdello group possessed the most rapid healing rate among all the groups.

The relative wound areas (Fig. 6c) decreased to 10.7 % of their initial areas in the ALP@Bdello group, whereas they decreased to 53.5 %, 31 %, 34.4 %, and 22.6 % in the PBS, Bdello, ALP, and ALP + Bdello groups, respectively. Besides, significant reduction of biofilm formation on the skin wound surface was observed in the ALP@Bdello group (Fig. 6d). Histomorphological analysis using HE and Mason staining (Fig. 6e) revealed nearly complete closure of wounds with substantial formation of normal epithelium in the ALP@Bdello group. In contrast, wounds in the other groups showed visible gaps and minimal new epithelial cell growth. Additionally, the expression of inflammatory factors at the wound site was evaluated, and found (Fig. 6f) that levels of IL-1 β , IL-6, and TNF- α were the lowest in the ALP@Bdello group among all treatment groups. These results demonstrate that ALP@Bdello effectively reduces bacterial biofilm adherence to infected wound surfaces within a complex physiological environment and promotes healing of infected wounds in diabetic mice.

Moreover, HE staining of the heart, liver, spleen, lung, and kidney indicated that the mice were in good condition (Fig. S13), confirming minimal toxicity of the ALP and Bdello combination in vivo. In recent years, the biosafety of *B. bacteriovorus* has been recognized, studies in cell lines and animal models show that *B. bacteriovorus* exhibits no obvious toxicity and almost does not induce inflammatory responses [14,58,59]. Moreover, it is found in the intestines of healthy humans, with its abundance decreasing in disease states such as Inflammatory Bowel Diseases and Celiac disease [60]. Therefore, *B. bacteriovorus* is considered to have the potential to be used as an intestinal probiotic to regulate gut disorders and restore gut ecological balance.

Based on the experimental results, the immune response trigger by the introduction of ALP@Bdello in host is negligible. However, given that *B. bacteriovorus* is a predator of Gram-negative bacteria, minimizing the effect of ALP@Bdello on beneficial Gram-negative bacteria in the host microbiome is indeed an important consideration. The precise use of engineered *B. bacteriovorus* can effectively minimize its impact on the host microbiome. The application of engineered *B. bacteriovorus* should be carried out under specific conditions. The ALP@Bdello constructed in this study mainly targets biofilm-related diseases, such as implant infections, dental caries, and chronic infections in diabetic wounds. These diseases are often associated with persistent bacterial biofilm infections, especially in areas where stable biofilms form (e.g., wound surfaces, dental surfaces). In these cases, localized application of ALP@Bdello can effectively remove biofilms to control infections. Compared to systemic administration, localized use can minimize the potential impact on other beneficial Gram-negative probiotics in the host microbiome. In addition to localized applications, we have also considered potential challenges in future applications. To minimize interference with the host microbiome, a rational engineered *B. bacteriovorus* strategy is crucial. For example, the proper drug loading within the ALP@Bdello “backpack” and the dosage of *B. bacteriovorus* must be strictly controlled to ensure it acts at the target site while minimizing its impact on the overall microbiome. In addition, the combined use of probiotics or prebiotics may can maintain the diversity of the skin, oral, or intestinal microbiomes, thereby preserving the balance of the microbiota. However, this treatment should be specific, as microbiome changes vary among individuals during treatment. Monitoring and evaluation should be conducted, with personalized interventions to supplement the appropriate probiotics and prebiotics. This combination therapy may help reduce the risk of dysbiosis and maintain the health of the host microbiome.

4. Conclusion

In this study, we address the challenge of poor drug diffusion within biofilm by developing an ampicillin-encapsulated liposome modified *B. bacteriovorus* (ALP@Bdello) as a drug delivery and treatment approach for biofilm-related diseases. The predator *B. bacteriovorus* preys on Gram-negative bacteria and can penetrate and disrupt the dense structure of Gram-positive bacterial biofilms. During this process,

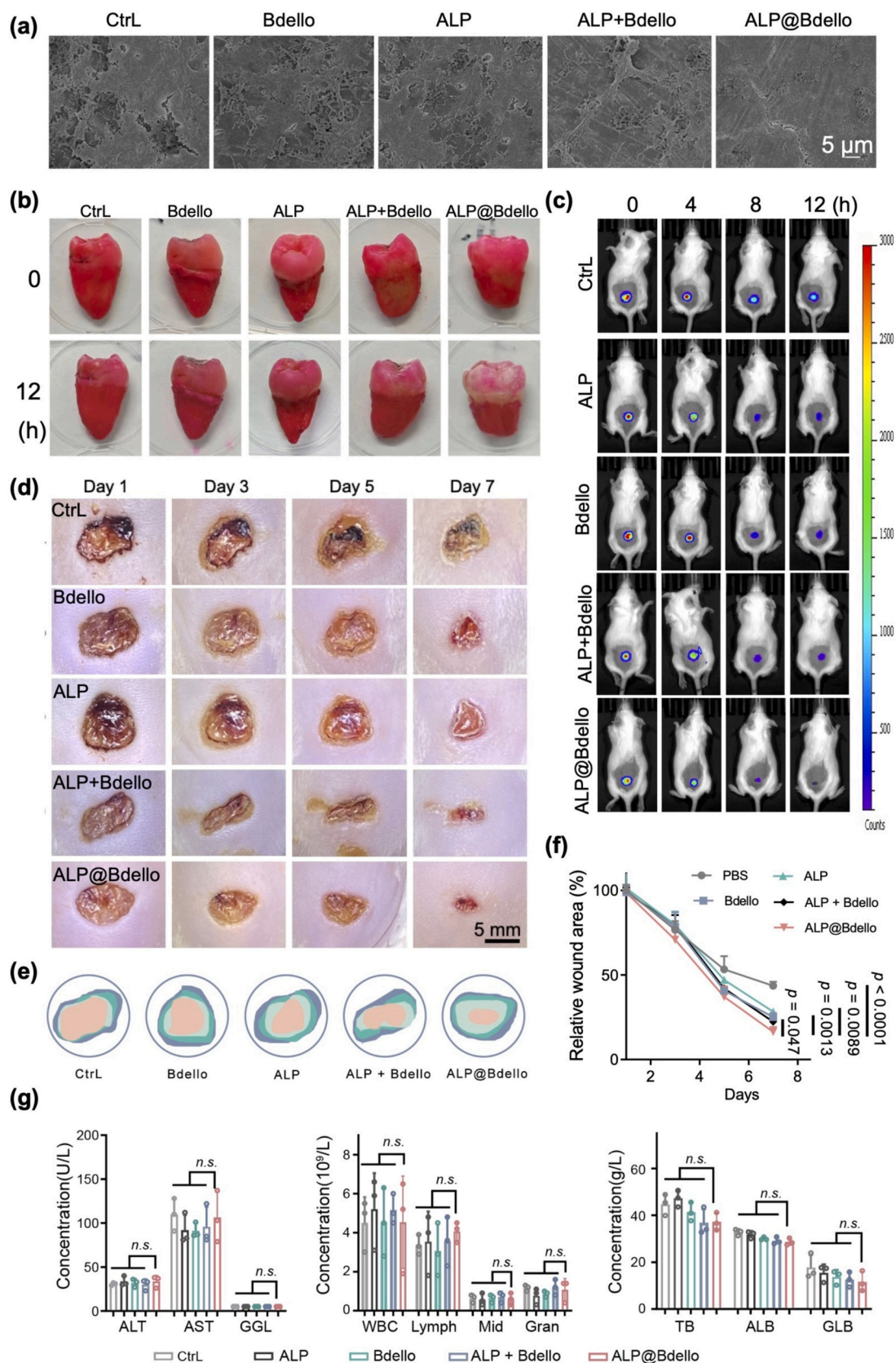


Fig. 5. Antibiofilm effects of ALP@Bdello on tooth and mice skin wounds. (a) Antibiofilm efficiency of ALP@Bdello against *S. mutans* biofilm formed on tooth slices. (b) Antibiofilm efficiency of ALP@Bdello on dental plaque biofilm. (c) Inhibitory effects of Bdello, ALP, ALP + Bdello, or ALP@Bdello on bioluminescent *E. coli* inoculated on mice skin wounds. (d–e) Therapeutic effects of PBS, Bdello, ALP, ALP + Bdello, and ALP@Bdello on *E. coli* and *S. aureus* co-infected skin wounds. (f) Relative wound area calculated by Image J based on digital images. (g) Blood biochemistry and blood routine analyses of mice with wounds treated with different materials.

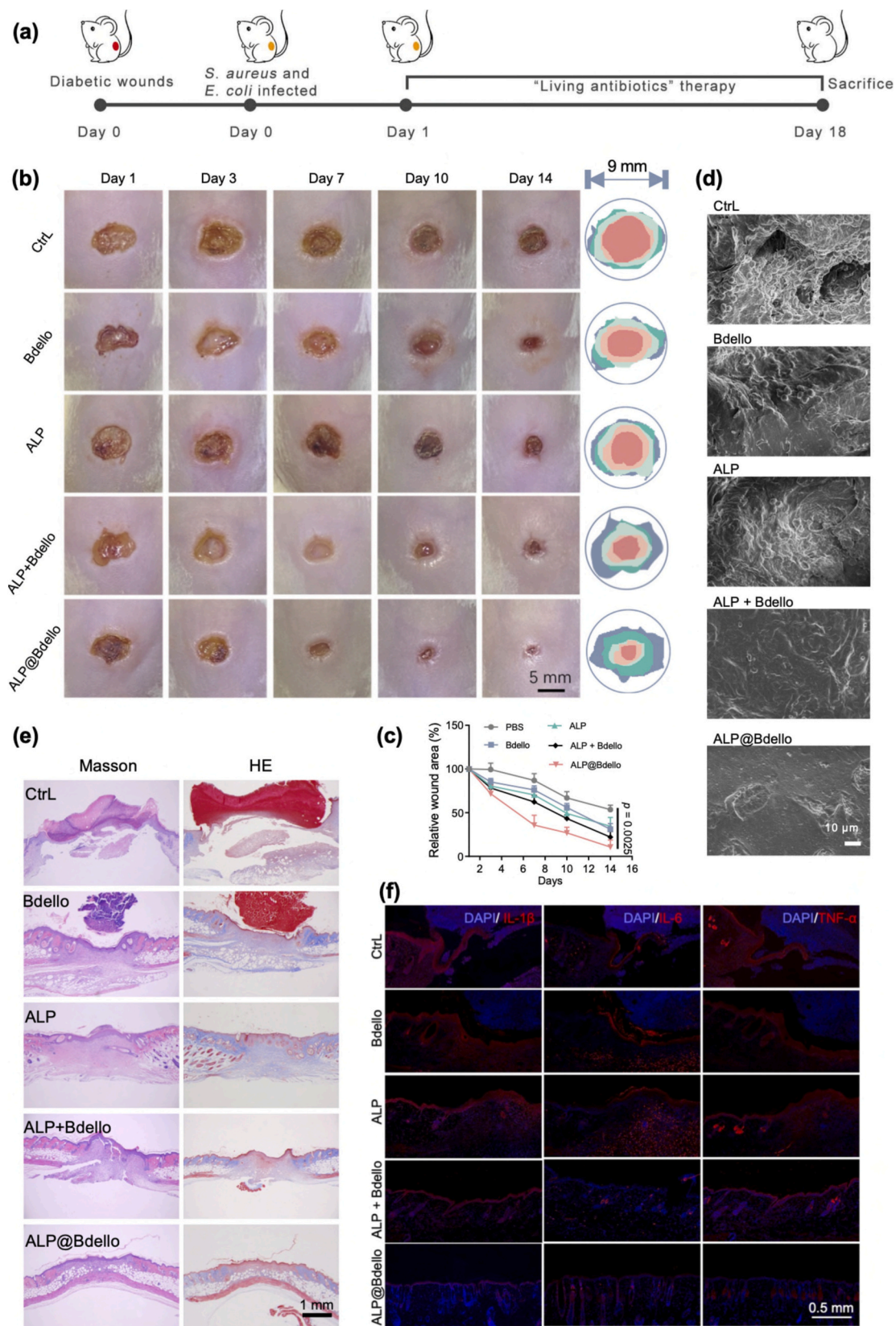


Fig. 6. Antibiofilm effects of ALP@Bdello on diabetic mice skin wounds. (a) Schematic diagram of experimental design and treatment process of diabetic wounds. (b) Therapeutic effects of PBS, Bdello, ALP, ALP + Bdello, and ALP@Bdello on *E. coli* and *S. aureus* co-infected skin wounds. (c) Relative wound area measured by Image J based on digital images. (d) SEM images of the wound surfaces with bacterial biofilm on day 14. (e) HE and Masson staining of the skin wound area. (f) Immunofluorescence staining of cell nucleus (DAPI) and inflammation markers (IL-1β, IL-6, and TNF-α) in wound tissue.

ALP@Bdello effectively delivers antibiotic-loaded liposomes into the biofilm, thereby enhancing the antibiotic release and improving biofilm eradication. Engineering *B. bacteriovorus* with antibiotic-encapsulated liposomes (ALP@Bdello) has proven to be more effective than the simpler hybrid approach of combining liposomes and *B. bacteriovorus*. This highlights the advantages of ALP@Bdello in penetrating biofilms and facilitating drug delivery. Both in vivo and in vitro results confirm that ALP@Bdello exhibits strong efficacy against both Gram-negative and Gram-positive biofilms, accelerating dental plaque removal and promoting the healing of infectious wounds. Additionally, liposomes are a well-established and widely utilized drug delivery system. The *B. bacteriovorus*-based delivery method shows potential for accommodating a variety of drugs, positioning it as a promising universal strategy for treating biofilm infections.

CRedit authorship contribution statement

Ying Tang: Writing – review & editing, Writing – original draft, Software, Methodology, Funding acquisition, Data curation. **Yang Chen:** Writing – review & editing, Writing – original draft, Software, Methodology, Data curation. **Yong-Dan Qi:** Writing – review & editing, Methodology, Data curation. **Hui-Yi Yan:** Writing – review & editing, Methodology. **Wen-An Peng:** Writing – review & editing, Methodology. **Yu-Qiang Wang:** Methodology. **Qian-Xiao Huang:** Methodology. **Xin-Hua Liu:** Writing – review & editing. **Jing-Jie Ye:** Writing – review & editing. **Yun Yu:** Writing – review & editing. **Xian-Zheng Zhang:** Writing – review & editing, Supervision, Project administration, Investigation, Funding acquisition, Formal analysis, Conceptualization. **Cui Huang:** Writing – review & editing, Supervision, Project administration, Investigation, Funding acquisition, Formal analysis, Conceptualization.

Declaration of competing interest

The authors declare that they have no known competing financial interests or personal relationships that could have appeared to influence the work reported in this paper.

Data availability

Data will be made available on request.

Acknowledgments

This work was supported by National Key Research and Development Program of China (2019YFA0905603), National Natural Science Foundation of China (22135005, 51833007, 82271010 and 82301154), Fundamental Research Funds for the Central Universities (2042023kf0149), and The Interdisciplinary Research Project of School of Stomatology Wuhan University (XNJ202307).

Appendix A. Supplementary data

Supplementary data to this article can be found online at <https://doi.org/10.1016/j.jconrel.2025.01.075>.

References

- J. Hurlow, R.D. Wolcott, P.G. Bowler, Clinical management of chronic wound infections: the battle against biofilm, *Wound Repair Regen.* 33 (2024) e13241.
- N.S. Jakubovics, S.D. Goodman, L. Mashburn-Warren, G.P. Stafford, F. Cieplik, The dental plaque biofilm matrix, *Periodontol* 2000 (86) (2021) 32–56.
- A. Uberoi, A. McCready-Vangi, E.A. Grice, The wound microbiota: microbial mechanisms of impaired wound healing and infection, *Nat. Rev. Microbiol.* 22 (2024) 507–521.
- World Health Organization, Antimicrobial Resistance: Global Report on Surveillance[M], World Health Organization, 2014.
- H.C. Flemming, J. Wingender, U. Szewzyk, P. Steinberg, S.A. Rice, S. Kjelleberg, Biofilms: An emergent form of bacterial life, *Nat. Rev. Microbiol.* 14 (2016) 563–575.
- M. Qin, X. Zhang, H. Ding, Y. Chen, W. He, Y. Wei, W. Chen, Y.K. Chan, Y. Shi, D. Huang, Y. Deng, Engineered probiotic bio-heterojunction with robust antibiofilm modality via “eating” extracellular polymeric substances for wound regeneration, *Adv. Mater.* 36 (2024) 2402530.
- D. Prantanto, C.K. Yeo, Y. Wu, C. Fan, X. Xu, Y.S. Yip, M.I.G. Vos, S. H. Mahadevowda, P.L.K. Lim, L. Yang, P.T. Hammond, D.I. Leavesley, N.S. Tan, M.B. Chan-Park, Hydrogel dressings with intrinsic antibiofilm and antioxidative dual functionalities accelerate infected diabetic wound healing, *Nat. Commun.* 15 (2024) 954.
- W. Cai, Y. Song, Q. Xie, S. Wang, D. Yin, S. Wang, S. Wang, R. Zhang, M. Lee, J. Duan, X. Zhang, Dual osmotic controlled release platform for antibiotics to overcome antimicrobial-resistant infections and promote wound healing, *J. Control. Release* 375 (2024) 627–642.
- W. Zhong, S. Handschuh-Wang, U.T. Uthappa, J. Shen, M. Qiu, S. Du, B. Wang, Miniature robots for battling bacterial infection, *ACS Nano* 18 (2024) 32335–32363.
- H. Peng, I.A. Chen, U. Qimron, Engineering phages to fight multidrug-resistant bacteria, *Chem. Rev.* (2024), <https://doi.org/10.1021/acs.chemrev.4c00681>.
- H. Stolp, M.P. Starr, Bdellovibrio bacteriovorus gen. et sp. n., a predatory, ectoparasitic, and bacteriolytic microorganism, *Antonie Van Leeuwenhoek* 29 (1963) 217–248.
- K. Plaskowska, J. Zakrzewska-Czerwińska, Chromosome structure and DNA replication dynamics during the life cycle of the predatory bacterium Bdellovibrio bacteriovorus, *FEMS Microbiol. Rev.* 47 (2023) fuad057.
- E. Marine, D.S. Milner, C. Lambert, R.E. Sockett, K.M. Pos, A novel method to determine antibiotic sensitivity in Bdellovibrio bacteriovorus reveals a DHFR-dependent natural trimethoprim resistance, *Sci. Rep.* 10 (2020) 5315.
- D. Negus, C. Moore, M. Baker, D. Raghunathan, J. Tyson, R.E. Sockett, Predator versus pathogen: how does predatory Bdellovibrio bacteriovorus interface with the challenges of killing gram-negative pathogens in a host setting? *Ann. Rev. Microbiol.* 71 (2017) 441–457.
- F.M. Cavallo, L. Jordana, A.W. Friedrich, C. Glasner, J.M. van Dijk, Bdellovibrio bacteriovorus: a potential ‘living antibiotic’ to control bacterial pathogens, *Crit. Rev. Microbiol.* 47 (2021) 630–646.
- F. Pantanella, V. Iebba, F. Mura, L. Dini, V. Totino, B. Neroni, G. Bonfiglio, M. Trancassini, C. Passariello, S. Schippa, Behaviour of Bdellovibrio bacteriovorus in the presence of Gram-positive Staphylococcus aureus, *New Microbiol.* 41 (2018) 145–152.
- M. Waso-Reyneke, S. Khan, W. Khan, Interaction of Bdellovibrio bacteriovorus with gram-negative and gram-positive bacteria in dual species and polymicrobial communities, *Microorganisms* 10 (2022) 793.
- H. Im, M. Dwidar, R.J. Mitchell, Bdellovibrio bacteriovorus HD100, a predator of Gram-negative bacteria, benefits energetically from Staphylococcus aureus biofilms without predation, *ISME J.* 12 (2018) 2090–2095.
- Z. Mohsenipour, P. Arazi, M. Skurnik, B. Jahanbin, H.R. Abtahi, M. Edalatfard, M. M. Feizabadi, Predation on bacterial pathogens by predatory bacteria of sewage origin: three days prey-predator interactions, *BMC Microbiol.* 24 (2024) 516.
- A.K. Monnappa, W. Bari, S.Y. Choi, R.J. Mitchell, Investigating the responses of human epithelial cells to predatory bacteria, *Sci. Rep.* 6 (2016) 33485.
- S. Gupta, C. Tang, M. Tran, D.E. Kadouri, Effect of predatory bacteria on human cell lines, *PLoS One* 11 (2016) e0161242.
- A.R. Willis, C. Moore, M. Mazon-Moya, S. Krokowski, C. Lambert, R. Till, S. Mostowy, R.E. Sockett, Injections of predatory bacteria work alongside host immune cells to treat Shigella infection in zebrafish larvae, *Curr. Biol.* 26 (2016) 3343–3351, <https://doi.org/10.1016/j.cub.2016.09.067>.
- W. Mun, S.Y. Choi, S. Upatissa, R.J. Mitchell, Predatory bacteria as potential biofilm control and eradication agents in the food industry, *Food Sci. Biotechnol.* 32 (2023) 1729–1743.
- K. Alexakis, S. Baliou, P. Ioannou, Predatory bacteria in the treatment of infectious diseases and beyond, *Infect. Dis. Rep.* 16 (2024) 684–698.
- D.W. Zheng, R.Q. Li, J.X. An, T.Q. Xie, Z.Y. Han, R. Xu, Y. Fang, X.Z. Zhang, Prebiotics-encapsulated probiotic spores regulate gut microbiota and suppress colon cancer, *Adv. Mater.* 32 (2020) 2004529.
- Z. Cao, Y. Pang, J. Pu, J. Liu, Bacteria-based drug delivery for treating non-oncological diseases, *J. Control. Release* 366 (2024) 668–683.
- P. Guo, S. Wang, H. Yue, X. Zhang, G. Ma, X. Li, W. Wei, Advancement of engineered bacteria for orally delivered therapeutics, *Small* 19 (2023) e2302702.
- H. Jiang, Z. Cao, Y. Liu, R. Liu, Y. Zhou, J. Liu, Bacteria-based living probes: preparation and the applications in bioimaging and diagnosis, *Adv. Sci.* 11 (2024) e2306480.
- Y. Tang, Q.X. Huang, D.W. Zheng, Y. Chen, L. Ma, C. Huang, X.Z. Zhang, Engineered Bdellovibrio bacteriovorus: a countermeasure for biofilm-induced periodontitis, *Mater. Today* 53 (2022) 71–83.
- H. Cao, S. He, H. Wang, S. Hou, L. Lu, X. Yang, Bdellovibrios, potential biocontrol bacteria against pathogenic *Aeromonas hydrophila*, *Vet. Microbiol.* 154 (2012) 413–418.
- H. Chen, Y. Cheng, J. Tian, P. Yang, X. Zhang, Y. Chen, Y. Hu, J. Wu, Dissolved oxygen from microalgae-gel patch promotes chronic wound healing in diabetes, *Sci. Adv.* 6 (2020) eaba4311.
- T. Ji, J. Lang, J. Wang, R. Cai, Y. Zhang, F. Qi, L. Zhang, X. Zhao, W. Wu, J. Hao, Z. Qin, Y. Zhao, G. Nie, Designing liposomes to suppress extracellular matrix expression to enhance drug penetration and pancreatic tumor therapy, *ACS Nano* 11 (2017) 8668–8678.

- [33] S. Dharani, D.H. Kim, R.M.Q. Shanks, Y. Doi, D.E. Kadouri, Susceptibility of colistin-resistant pathogens to predatory bacteria, *Res. Microbiol.* 169 (2018) 52–55.
- [34] H. Stolp, The Bdellovibrion: bacterial parasites of bacteria, *Annu. Rev. Phytopathol.* 11 (1973) 53–76.
- [35] H. Stolp, Interactions between Bdellovibrio and its host cell, *Proc. R. Soc. Lond. B* 204 (1979) 211–217.
- [36] E. Jurkevitch, Predatory behaviors in Bacteria-diversity and transitions, *Microbe Mag.* 2 (2007) 67–73.
- [37] D.E. Large, R.G. Abdelmessih, E.A. Fink, D.T. Auguste, Liposome composition in drug delivery design, synthesis, characterization, and clinical application, *Adv. Drug Deliv. Rev.* 176 (2021) 113851.
- [38] J. Di, F. Xie, Y. Xu, When liposomes met antibodies: drug delivery and beyond, *Adv. Drug Deliv. Rev.* 154–155 (2020) 151–162.
- [39] S.G. Antimisiaris, A. Marazioti, M. Kannavu, E. Natsaridis, F. Gkartziou, G. Kogkos, S. Mourtas, Overcoming barriers by local drug delivery with liposomes, *Adv. Drug Deliv. Rev.* 174 (2021) 53–86.
- [40] S.H.E. Kaufmann, A. Dorhoi, R.S. Hotchkiss, R. Bartenschlager, Host-directed therapies for bacterial and viral infections, *Nat. Rev. Drug Discov.* 17 (2018) 35–56.
- [41] F. Pimenta, A.C. Abreu, L.C. Simões, M. Simões, What should be considered in the treatment of bacterial infections by multi-drug therapies: a mathematical perspective? *Drug Resist. Updat.* 17 (2014) 51–63.
- [42] M.A. Trebino, R.D. Shingare, J.B. Macmillan, F.H. Yildiz, Strategies and approaches for discovery of small molecule disruptors of biofilm physiology, *Molecules* 26 (2021) 4582.
- [43] R.C. Lowrencea, S.G. Subramaniapillaib, V. Ulaganathanc, S. Nagarajan, Tackling drug resistance with efflux pump inhibitors: from bacteria to cancerous cells, *Crit. Rev. Microbiol.* 45 (2019) 334–353.
- [44] M. Miethke, M. Pieroni, T. Weber, M. Brönstrup, P. Hammann, L. Halby, P. B. Arimondo, P. Glaser, B. Aigle, H.B. Bode, R. Moreira, Y. Li, A. Luzhetskyy, M. H. Medema, J.L. Pernodet, M. Stadler, J.R. Tormo, O. Genilloud, A.W. Truman, K. J. Weissman, E. Takano, S. Sabatini, E. Stegmann, H. Brötz-Oesterhelt, W. Wohlleben, M. Seemann, M. Empting, A.K.H. Hirsch, B. Loretz, C.M. Lehr, A. Titz, J. Herrmann, T. Jaeger, S. Alt, T. Hestekamp, M. Winterhalter, A. Schiefer, K. Pfarr, A. Hoerauf, H. Graz, M. Graz, M. Lindvall, S. Ramurthy, A. Karlén, M. van Dongen, H. Petkovic, A. Keller, F. Peyrane, S. Donadio, L. Fraisse, L.J.V. Piddock, I. H. Gilbert, H.E. Moser, R. Müller, Towards the sustainable discovery and development of new antibiotics, *Nat. Rev. Chem.* 5 (2021) 726–749.
- [45] K. Kasza, P. Gurnani, K.R. Hardie, M. Cámara, C. Alexander, Challenges and solutions in polymer drug delivery for bacterial biofilm treatment: a tissue-by-tissue account, *Adv. Drug Deliv. Rev.* 178 (2021) 113973.
- [46] S. Subramaniam, P. Joyce, N. Thomas, C.A. Prestidge, Bioinspired drug delivery strategies for repurposing conventional antibiotics against intracellular infections, *Adv. Drug Deliv. Rev.* 177 (2021) 113948.
- [47] C. Lambert, K.J. Evans, R. Till, L. Hobley, M. Capeness, S. Rendulic, S.C. Schuster, S.I. Aizawa, R.E. Sockett, Characterizing the flagellar filament and the role of motility in bacterial prey-penetration by Bdellovibrio bacteriovorus, *Mol. Microbiol.* 60 (2006) 274–286.
- [48] S.F. Koval, M.E. Bayer, Bacterial capsules: no barrier against Bdellovibrio, *Microbiology* 143 (3) (1997) 749–753.
- [49] R. Sathyamoorthy, A. Maoz, Z. Pasternak, H. Im, A. Huppert, D. Kadouri, E. Jurkevitch, Bacterial predation under changing viscosities, *Environ. Microbiol.* 21 (2019) 2997–3010.
- [50] C. Lambert, A.K. Fenton, L. Hobley, R.E. Sockett, Predatory Bdellovibrio bacteria use gliding motility to scout for prey on surfaces, *J. Bacteriol.* 193 (2011) 3139–3141.
- [51] S. Rendulic, P. Jagtap, A. Rosinus, M. Eppinger, C. Baar, C. Lanz, H. Keller, C. Lambert, K.J. Evans, A. Alexander Goesmann, F. Meyer, R.E. Sockett, S. C. Schuster, A predator unmasked: life cycle of Bdellovibrio bacteriovorus from a genomic perspective, *Science* 303 (2004) (2004) 689–692.
- [52] C.W. Hall, T.F. Mah, Molecular mechanisms of biofilm-based antibiotic resistance and tolerance in pathogenic bacteria, *FEMS Microbiol. Rev.* 41 (2017) 276–301.
- [53] S.M. Moskowitz, J.M. Foster, J. Emerson, J.L. Burns, Clinically feasible biofilm susceptibility assay for isolates of Pseudomonas aeruginosa from patients with cystic fibrosis, *J. Clin. Microbiol.* 42 (2004) 1915–1922.
- [54] M. Waso, S. Khan, W. Ahmed, W. Khan, Expression of attack and growth phase genes of Bdellovibrio bacteriovorus in the presence of Gram-negative and Gram-positive prey, *Microbiol. Res.* 235 (2020) 126437.
- [55] V. Iebba, V. Totino, F. Santangelo, A. Gagliardi, L. Ciotoli, A. Virga, C. Ambrosi, M. Pompili, R.V. De Biase, L. Selan, M. Artini, F. Pantanella, F. Mura, C. Passariello, M. Nicoletti, L. Nencioni, M. Trancassini, S. Quattrucci, S. Schippa, Bdellovibrio bacteriovorus directly attacks Pseudomonas aeruginosa and Staphylococcus aureus cystic fibrosis isolates, *Front. Microbiol.* 5 (2014) 280.
- [56] L.J. Bessa, P. Fazzi, M. Di Giulio, L. Cellini, Bacterial isolates from infected wounds and their antibiotic susceptibility pattern: some remarks about wound infection, *Int. Wound J.* 12 (2015) 47–52.
- [57] K. Gjødsvøl, J.J. Christensen, T. Karlsmark, B. Jørgensen, B.M. Klein, K.A. Kroghfelt, Multiple bacterial species reside in chronic wounds: a longitudinal study, *Int. Wound J.* 3 (2006) 225–231.
- [58] A. Mookherjee, E. Jurkevitch, Interactions between Bdellovibrio and like organisms and bacteria in biofilms: beyond predator–prey dynamics, *Environ. Microbiol.* 24 (2022) 998–1011.
- [59] K. Shatzkes, R. Chae, C. Tang, G.C. Ramirez, S. Mukherjee, L. Tsenova, N. D. Connell, D.E. Kadouri, Examining the safety of respiratory and intravenous inoculation of Bdellovibrio bacteriovorus and Micavibrio aeruginosavorus in a mouse model, *Sci. Rep.* 5 (2015) 12899.
- [60] V. Iebba, F. Santangelo, V. Totino, M. Nicoletti, A. Gagliardi, R.V. De Biase, S. Cucchiara, L. Nencioni, M.P. Conte, S. Schippa, Higher prevalence and abundance of Bdellovibrio bacteriovorus in the human gut of healthy subjects, *PLoS One* 8 (2013) e61608.